Interpolation between the weak and strong coupling regimes in quenched QCD

Yannick Meurice
The University of Iowa
yannick-meurice@uiowa.edu

Continuous Advances in QCD, May 11 2006

Content of the talk

- I. We have hit some "walls" with perturbation theory

  ("wall" has a technical meaning that I will explain)

- II. Solution: an optimally chosen field cutoff

  (a few examples of calculations; the optimization uses the strong couping)

- III. The average plaquette in quenched lattice QCD
  - Complex singularities (off the real axis;no third order phase transition)
  - The controversial non-perturbative part

  (theses are parametrizations ; no modified pert. calculations so far)

I. Limitations of Perturbation Theory

- The experimental error bars of precision measurements have been shrinking (LEP, g-2) and a significant effort has been made to calculate higher order terms of perturbative series. Precision tests may become a major source of information regarding new laws of nature.

- In many QFT models, perturbative series have a zero radius of convergence (Dyson 1952).

- A common practice to estimate at which order, for a given coupling, we reach the maximal accuracy in perturbation theory is to determine when the ratio of successive contributions reaches one. This method works reasonably well for several examples where nonperturbative numerical results are available.

Quantity	*1990 Value* $(\times 10^{11})$	*2001 Value* $(\times 10^{11})$	*Change* $(\times 10^{11})$
$a_\mu^{\rm QED}$	116 584 695.5(5.4)	116 584 705.7(2.9)	$+10.2$
$a_\mu^{\rm Had}$ (vac. pol 1)	7 068(59)(164)	6 924(62)	-144
$a_\mu^{\rm Had}$ (vac. pol 2)	-90(5)	-100(6)	-10
$a_\mu^{\rm Had}$ (light by light)	49(5)	-85(25)	-134
$a_\mu^{\rm EW}$ (1 loop)	195(10)	195	0
$a_\mu^{\rm EW}$ (2 loop)	—	$-43(4)$	-43
$a_\mu^{\rm SM}$ (total)	116 591 918(176)	116 591 597(67)	-321

Table 1: Improvements in the theoretical calculation of a_μ from 1990 to 2001. The major shifts were primarily due to errors in the earlier calculations, new calculations of higher order effects, improved $e^+e^- \to$ hadrons and tau data, and additional utilization of perturbative QCD. (From W. Marciano, hep-ph/0105056)

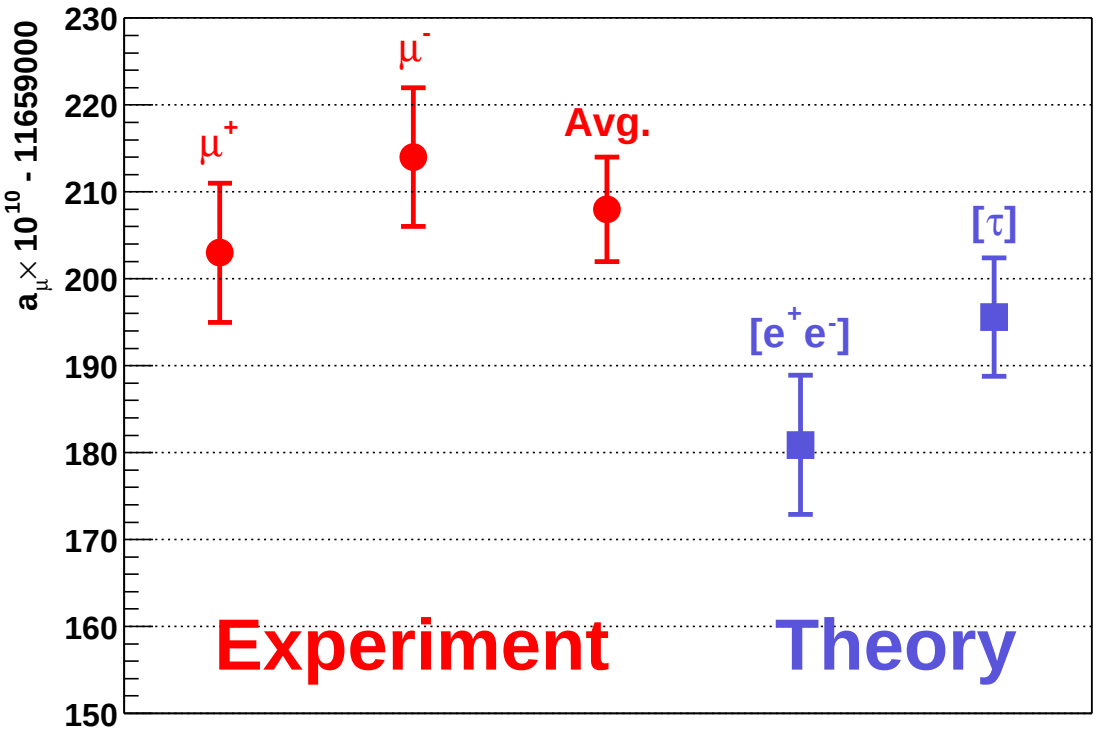

Figure 1: Measurements of a_μ by E821 with the SM predictions (Bennett et al., Phys. Rev. Lett. 92 161802 (2004); hep-ex/0401008).

- The problem is more serious in the case of perturbative QCD corrections. For instance, in the calculation (Larin et al. PLB 320 159 (1994)) of the hadronic width of the Z^0, the term of order α_s^3 is more than 60 percent of the term of order α_s^2 and contributes to one part in 1,000 to the total width (a typical experimental error at LEP).

- For NNLO corrections in LHC processes, see a recent talk of K. Ellis:

  http://theory.fnal.gov/people/ellis/Talks/wab.pdf

  We need new "recipes" ! (e.g. for the propagator with a field cut)

II. A possible cure (explained with a simple integral)

$$\int_{-\infty}^{+\infty} d\phi e^{-\frac{1}{2}\phi^2-\lambda\phi^4} \neq \sum_{0}^{\infty} \frac{(-\lambda)^l}{l!} \int_{-\infty}^{+\infty} d\phi e^{-\frac{1}{2}\phi^2} \phi^{4l} \tag{1}$$

The peak of the integrand of the r.h.s. moves too fast when the order increases (see next slide). On the other hand, if we introduce a field cutoff, the peak moves outside of the integration range and

$$\int_{-\phi_{max}}^{+\phi_{max}} d\phi e^{-\frac{1}{2}\phi^2-\lambda\phi^4} = \sum_{0}^{\infty} \frac{(-\lambda)^l}{l!} \int_{-\phi_{max}}^{+\phi_{max}} d\phi e^{-\frac{1}{2}\phi^2} \phi^{4l} \tag{2}$$

General expectations: for a finite lattice, the partition function Z calculated with a field cutoff is convergent and $\ln(Z)$ has a finite radius of convergence.

Effect of a field cutoff

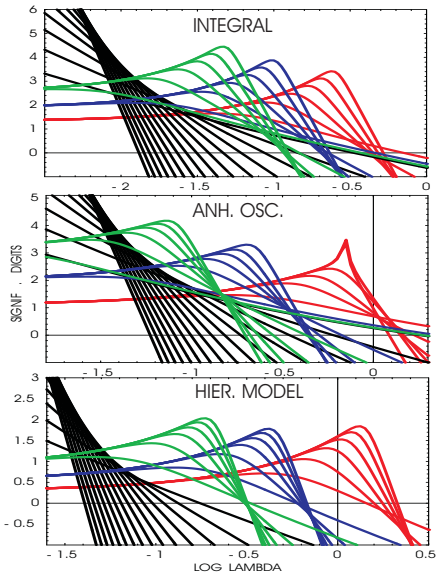

Figure 2: Significant digits obtained with regular perturbation theory at odd orders (black) and with $\phi_{max} = 3$ (green), 2.5 (blue) and 2 (red), for the integral, the ground state energy of the anh. osc and the renormalized mass of Dyson's model (see YM PRL 88 141601 (2002) for details).

Optimization

- We can adjust $\phi_{max}(\lambda, K)$ in order to minimize or eliminate the discrepancy with the (usually unknown) correct value. As ϕ_{max} is varied, the curve (or the derivative) of the approximate expression crosses the numerical curve (or its derivative).

- The strong coupling can be used to calculate approximately this optimal $\phi_{max}(\lambda, K)$ (natural approach of a weak/strong coupling crossover)

- The perturbative "coefficients" $a_k(\phi_{max}(\lambda, K))$ now depend on λ.

see B. Kessler, L. Li and YM, PRD 69 045014 (2004).

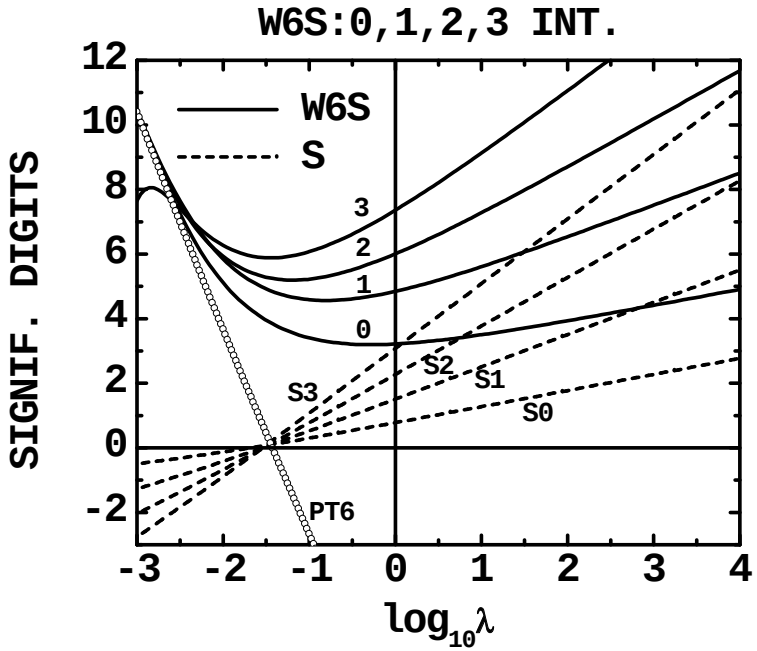

Figure 3: Significant digits obtained with the optimal cut $\phi_{max}(\lambda)$ (corresponding to a truncated expansion at order 6 in the weak coupling) estimated using the strong coupling expansion at orders 0, 1, 2 and 3 (solid lines), compared to significant digits using only the strong coupling expansion of the integral at the same orders in the strong coupling (dashed lines) and regular perturbation theory at order 6 (PT6).

Perturbative Calculations with a Field Cutoff

The calculation of the modified coefficients $a_k(\phi_{max})$ fall in three categories:

- Low k (the usual ones with exponentially small corrections; semi classical)
- Intermediate k (crossover; complicated but with universal features)
- Large k (power suppressed; no $k!$ behavior)

Examples: the anharmonic oscillator and $D = 3$ Dyson hierarchical model; see YM PRL 88 141601; Li and YM, JPA 38 8139 and in press

Intuitive flow picture

The beginning of the series corresponds to the behavior of the scaling variables near the gaussian fixed point.

The large order, corresponds to the approach of the high-temperature/strong-coupling fixed point.

The coefficients in the crossover (ϕ_{max} dependent) correspond to the crossover in the flows.

To be tested by constructing the gaussian scaling fields of the hierarchical model.

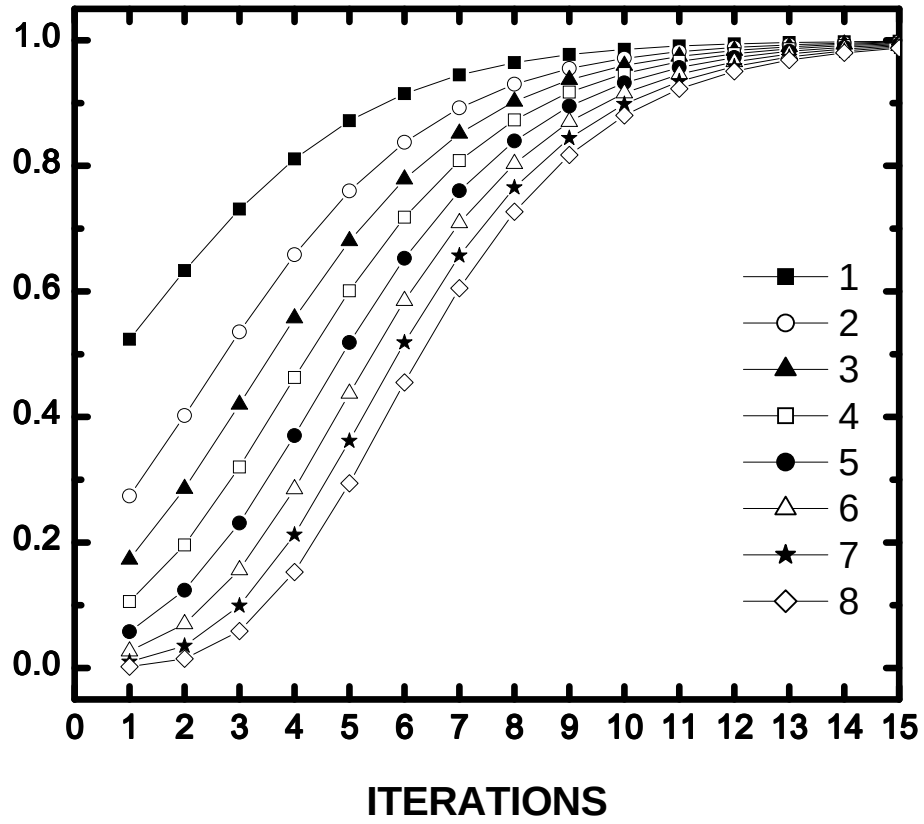

Figure 4: The first 8 perturbative coefficients (calculated with a field cut) of the zero-momentum two point function of the $D = 3$ hierarchical model, in units of their final values as a function of the number of iterations. As the cut decreases, the curves spread apart

1 plaquette LGT, (Li, YM PRD 71 054509 (2005))

$$Z(\beta, N) = \int \prod_{l \in p} dU_l \mathrm{e}^{-\beta(1-\frac{1}{N} ReTrU_p)} \ ,$$

$$Z(\beta, 2) = (2/\beta)^{3/2} \frac{1}{\pi} \int_0^{2\beta} dt t^{1/2} \mathrm{e}^{-t} \sqrt{1-(t/2\beta)}$$

$$Z(\beta, 2, t_{max}) = (2/\beta)^{3/2} \frac{1}{\pi} \int_0^{t_{max}} dt t^{1/2} \mathrm{e}^{-t} \sqrt{1-(t/2\beta)}$$

$$Z(\beta, 2, t_{max}) = (\beta\pi)^{-3/2} 2^{1/2} \sum_{l=0}^{\infty} A_l(t_{max}) (2\beta)^{-l} \ ,$$

with

$$A_l(t_{max}) \equiv \frac{\Gamma(l+1/2)}{l!(1/2-l)} \int_0^{t_{max}} dt \mathrm{e}^{-t} t^{l+1/2} \ ,$$

$$Z(\beta, t_{max}) = (\beta\pi)^{-3/2} 2^{1/2} \sum_{l=0}^{\infty} A_l(t_{max})(2\beta)^{-l} \ ,$$

$$A_l(t_{max}) \equiv \frac{\Gamma(l+1/2)}{l!(1/2-l)} \int_0^{t_{max}} dt \mathrm{e}^{-t} t^{l+1/2} \ ,$$

When $t_{max} \to \infty$ the integral becomes the (complete) Γ function and the coefficients grow factorially. In lattice perturbation theory, we "add the tails" (to make the calculation easier).

When t_{max} is finite, the integral is bounded by a power of t_{max}. When $t_{max} \leq 2\beta$, the sum converges.

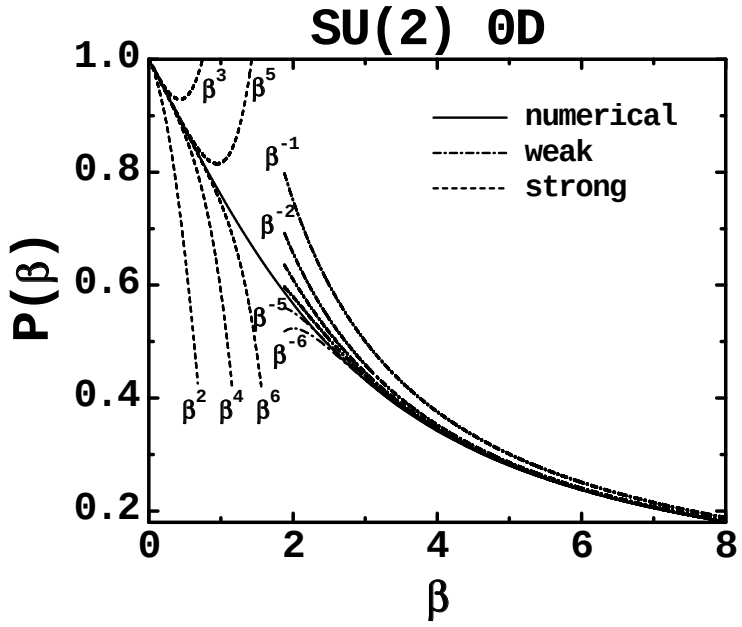

Figure 5: P versus β for $SU(2)$ on one plaquette. The solid line represents the numerical values; the dashed lines on the left, successive orders in the strong coupling expansion; the dot-dash lines on the right, successive order in the weak coupling expansion.

Regular PT (weak coupling on the right now)

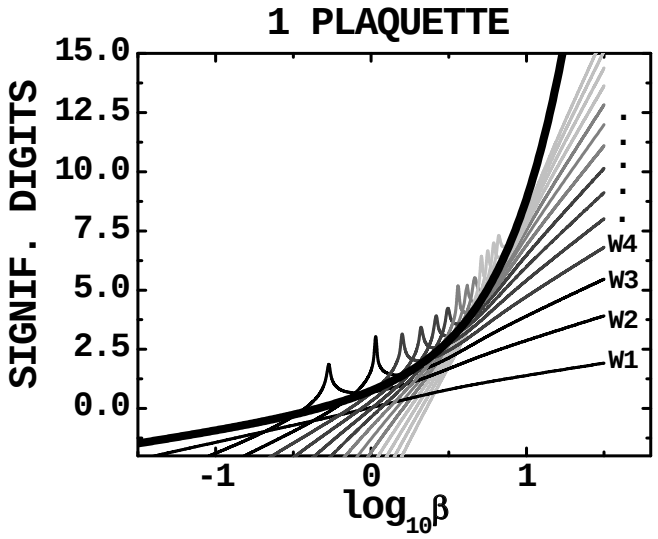

Figure 6: Number of correct significant digits as a function of β at successive orders of the regular perturbative series for $Z(\beta)$. As the order increases from 1 to 15, the curves $(W1,\ W2, \dots)$ get lighter. The thick solid line is $\log_{10}(\beta^{-1}\mathrm{e}^{-2\beta}/Z)$ ("instanton effect")

Optimized cut perturbation theory

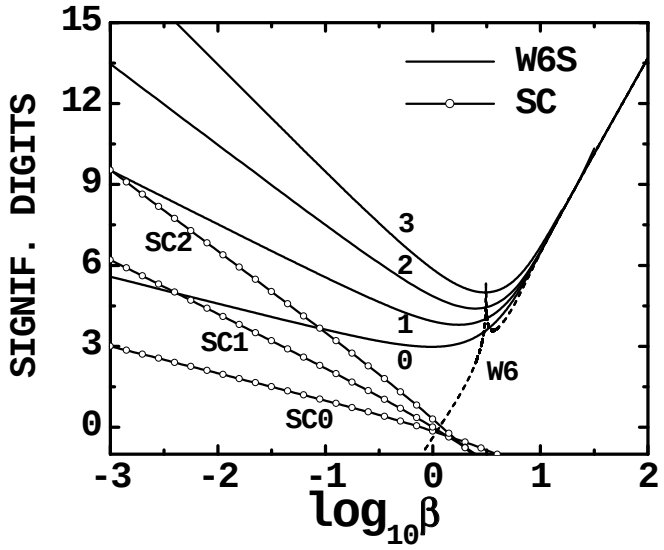

Figure 7: Significant digits obtained from the weak series truncated at order 6 using the first solution for t_{max}/β at order 0 to 3 compared to the weak coupling expansion at order 6 (dotted line W6) and the strong coupling expansion at order 0 to 2 (empty circles SC)

III Quenched lattice QCD

$$S = \beta \sum_{plaq.} (1 - (1/N) ReTr(U_p)) \ , \tag{3}$$

with $\beta = 2N/g^2$. The lattice functional integral or partition function is

$$Z = \prod_l \int dU_l \mathrm{e}^{-S} \tag{4}$$

with dU_l the $SU(N)$ invariant Haar measure for the group element associated with the link l.

$< \mathcal{O} >$ is defined by inserting $\mathcal{O}$ in the integral and dividing by Z. We consider symmetric (hypercubic) lattices with L^D sites and periodic boundary conditions.

The total number of 1×1 plaquettes is denoted

$$\mathcal{N}_p \equiv \ L^D D(D-1)/2 \ . \tag{5}$$

Using

$$f \equiv -(1/\mathcal{N}_p) \ln Z \ , \tag{6}$$

we define the average plaquette

$$\begin{aligned} P(\beta) &\equiv \partial f/\partial\beta \\ &= (1/\mathcal{N}_p) \left\langle \sum_p (1-(1/N) ReTr(U_p)) \right\rangle \ . \end{aligned} \tag{7}$$

and the specific heat $C_V = -\beta^2 \partial P/\partial\beta$.

Lattice Perturbation Theory

Three steps (Heller and Karsch, NPB 251 254)

1. $\beta = 2N/g^2$; $U = e^{igA}$ with $A = A^a T^a$

2. Extend the range of integration of the A^a from $-\infty$ to $+\infty$

3. Expand in g

We used the series of Di Renzo et al. JHEP 10 038 hep-lat/0011067.

$$P(1/\beta) = \sum_{m=0}^{10} b_m \beta^{-m} + \ldots .$$

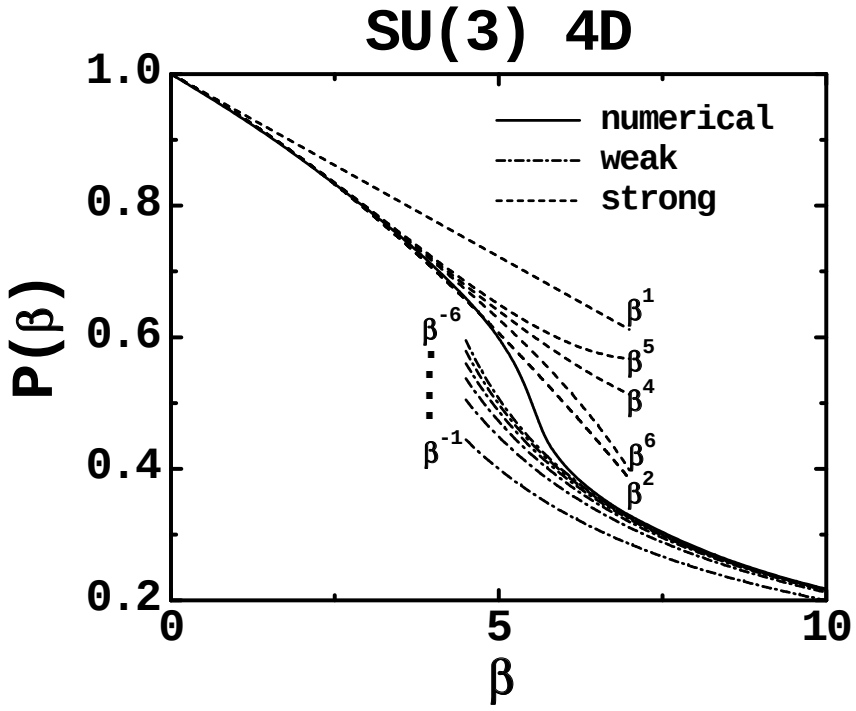

Figure 8: P versus β for $SU(3)$ in 4 dimensions. The solid line represents the numerical values; the dashed lines on the left, successive orders in the strong coupling expansion; the dot-dash lines on the right, successive orders in the weak coupling expansion.

Padé Approximants

Typically, "good" (weak) approximants have a pole near 5.2

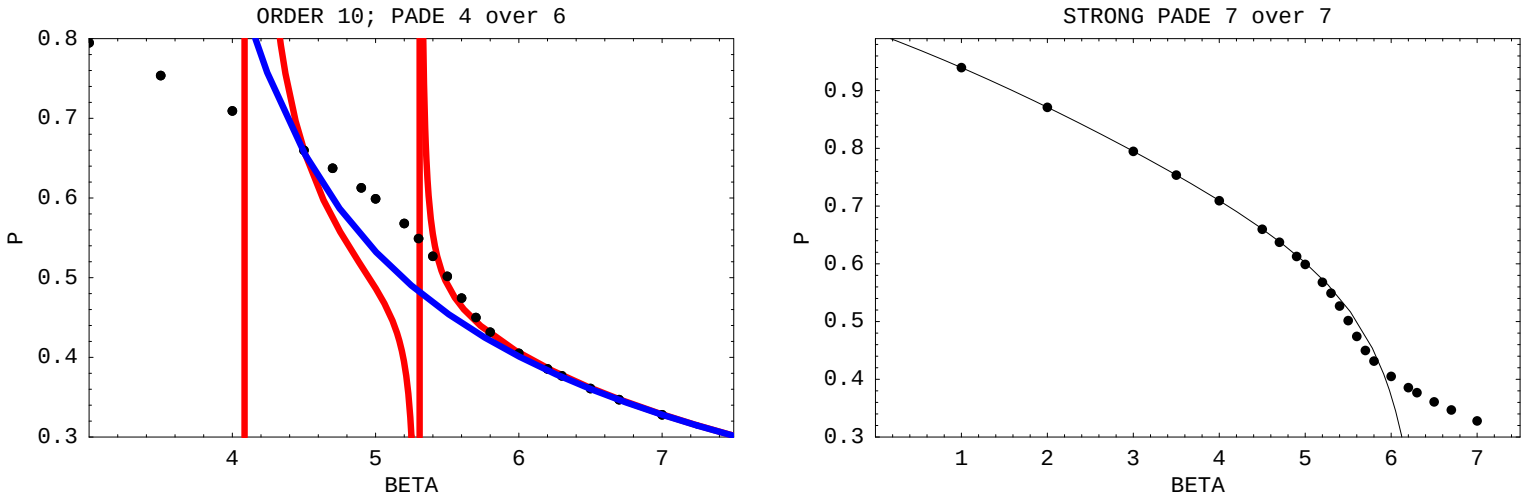

Figure 9: Regular weak series (blue) and 4/6 Padé (red) for the plaquette (left); Strong 7/2 Padé (right)

Series analysis (L. Li and Y. M. PRD D73 036006)

- $P \propto (1/5.74 - 1/\beta)^{1.08}$???
  - not expected (zero radius of convergence; no singularity between confinement and AF; no massless state)
  - good agreement with Horsley et al. hep-lat/0110210
  - could in principle be visible in 2d derivative of P (statistical errors permitting)

- Not incompatible with asymptotic series (P could be a superposition of a function that has an asymptotic series and one that has a finite radius of convergence) provided that the factorial behavior shows up at a large enough order.

Direct Search for Singularities in P' and P''

$$-\partial P/\partial\beta = (1/\mathcal{N}_p)[\langle\Sigma^2\rangle - \langle\Sigma\rangle^2] \ , \tag{8}$$

$$\partial^2 P/\partial\beta^2 = (1/\mathcal{N}_p)[\langle\Sigma^3\rangle - 3\,\langle\Sigma\rangle\,\langle\Sigma^2\rangle + \langle\Sigma\rangle^3] \tag{9}$$

Loss of precision in the calculation of the higher moments: in $-\partial P\partial\beta$, the two terms are of order $\mathcal{N}_p$ but their difference is of order 1. For 10^4 lattice, P'' will appear in the ninth significant digit and the use of double precision is crucial.

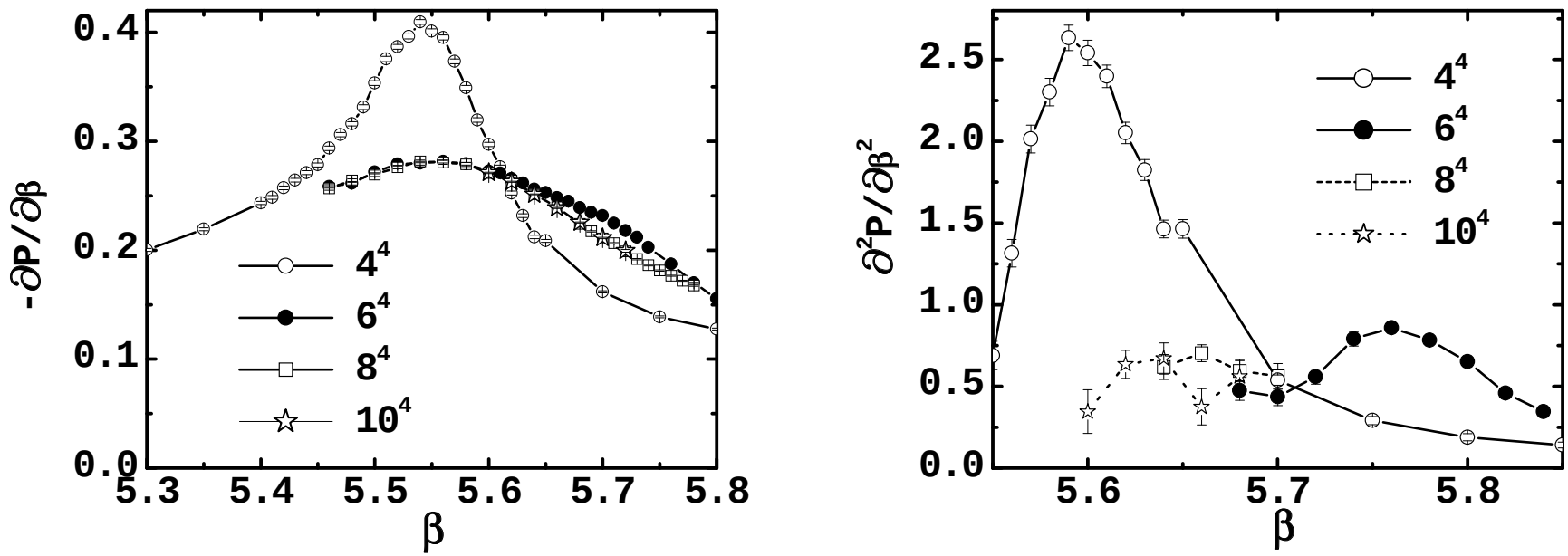

Figure 10: First and second derivative of P versus β on L^4 lattices.

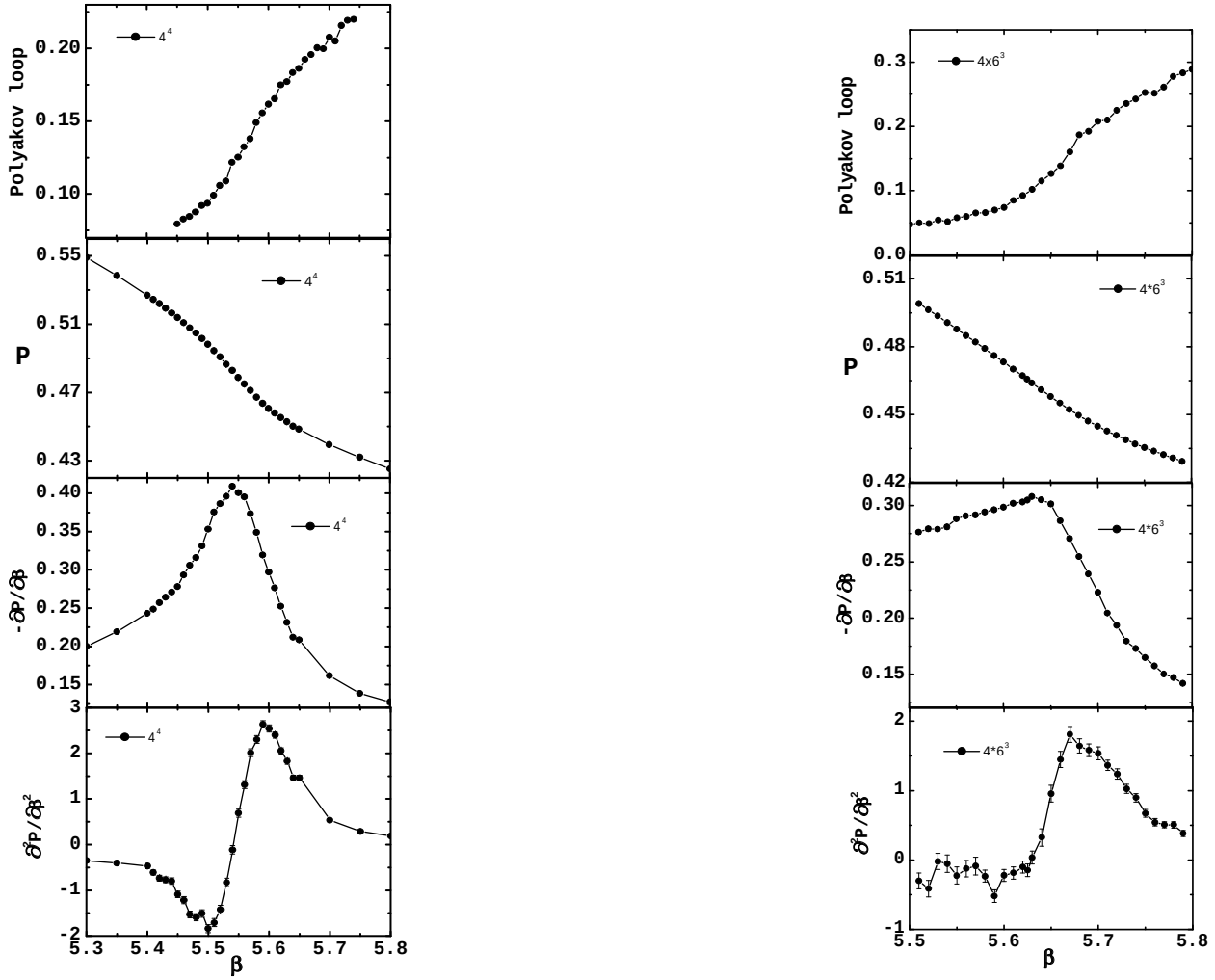

Figure 11: The Polyakov loop, P, first and second derivative of P versus β for 4^4 and 4×6^3 lattices .

A simple alternative can be designed by assuming that the critical point in the fundamental-adjoint plane has mean field exponents and in particular $\alpha = 0$. We will further assume an approximate logarithmic behavior

$$-\partial P/\partial\beta \propto \ln((1/\beta_m - 1/\beta)^2 + \Gamma^2) \ , \tag{10}$$

on the axis where the adjoint term of the action is zero (the range of parameters considered here). $1/\beta_m$ denotes the value where the argument of the logarithm is maximal on this axis. This implies the approximate form

$$\partial^2 P/\partial\beta^2 \simeq -C\frac{(1/\beta_m - 1/\beta)}{\beta^3((1/\beta_m - 1/\beta)^2 + \Gamma^2)} \tag{11}$$

The β^3 at the denominator ensures that the series starts at β^{-3}.

Fits: $\beta_m \simeq 5.78$, $\Gamma \simeq 0.006$, and $C \simeq 0.15$

The variations in the estimation of C (typically $|\delta C| \sim 0.01$) and β_m (typically $|\delta\beta_m| \sim 0.02$) are small. On the other hand, Γ varies more rapidly under changes of the weights in the χ^2 function. We found values of Γ between 0.003 and 0.007.

The stability of C and β_m can be used to set a lower bound on Γ. Given that the approximate form of $\partial^2 P/\partial\beta^2$ in Eq. (11) has extrema at $1/\beta = 1/\beta_m \pm \Gamma$. As we do not observe values larger than 0.3 near $\beta = 5.75$ we get the approximate bound

$$\frac{C}{2\beta_m^3\Gamma} < 0.3 \tag{12}$$

This implies the lower bound $\Gamma > 0.001$. On the other hand, large values of Γ are also excluded. We never found estimate close to 0.01.

Small window for a complex singularity

The imaginary part Γ of the location of the singularity in the $1/\beta = g^2/6$ plane should be in the range

$$0.001 < \Gamma < 0.01 \ . \tag{13}$$

This suggests zeroes of the partition function in the complex β plane with

$$0.001\beta_m^2 < Im\beta < 0.01\beta_m^2 \simeq 0.33 \tag{14}$$

tested!

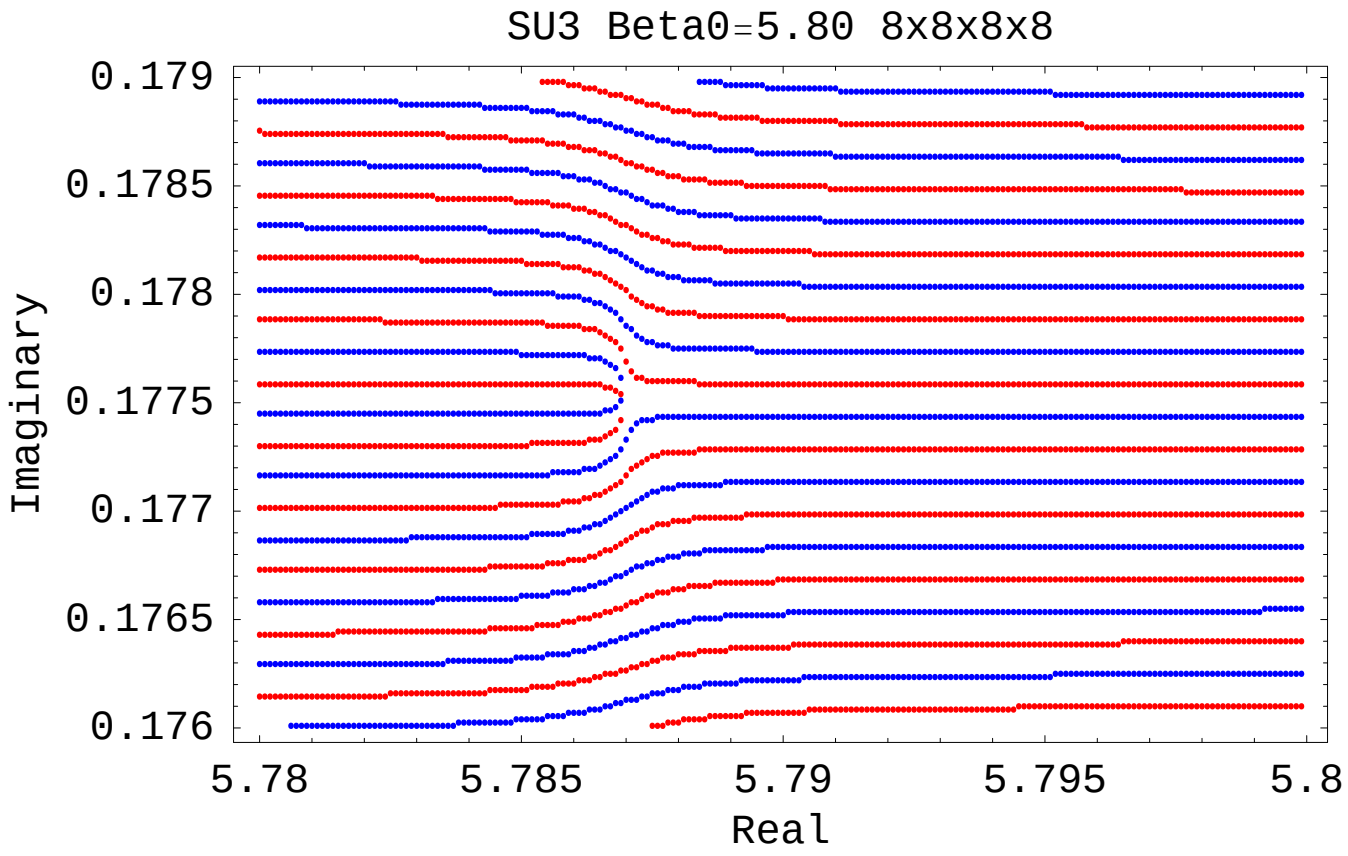

Figure 12: Zeroes of the real (blue) and imaginary (red) part of the partition function in the complex β plane (work done with Alan denBleyker).

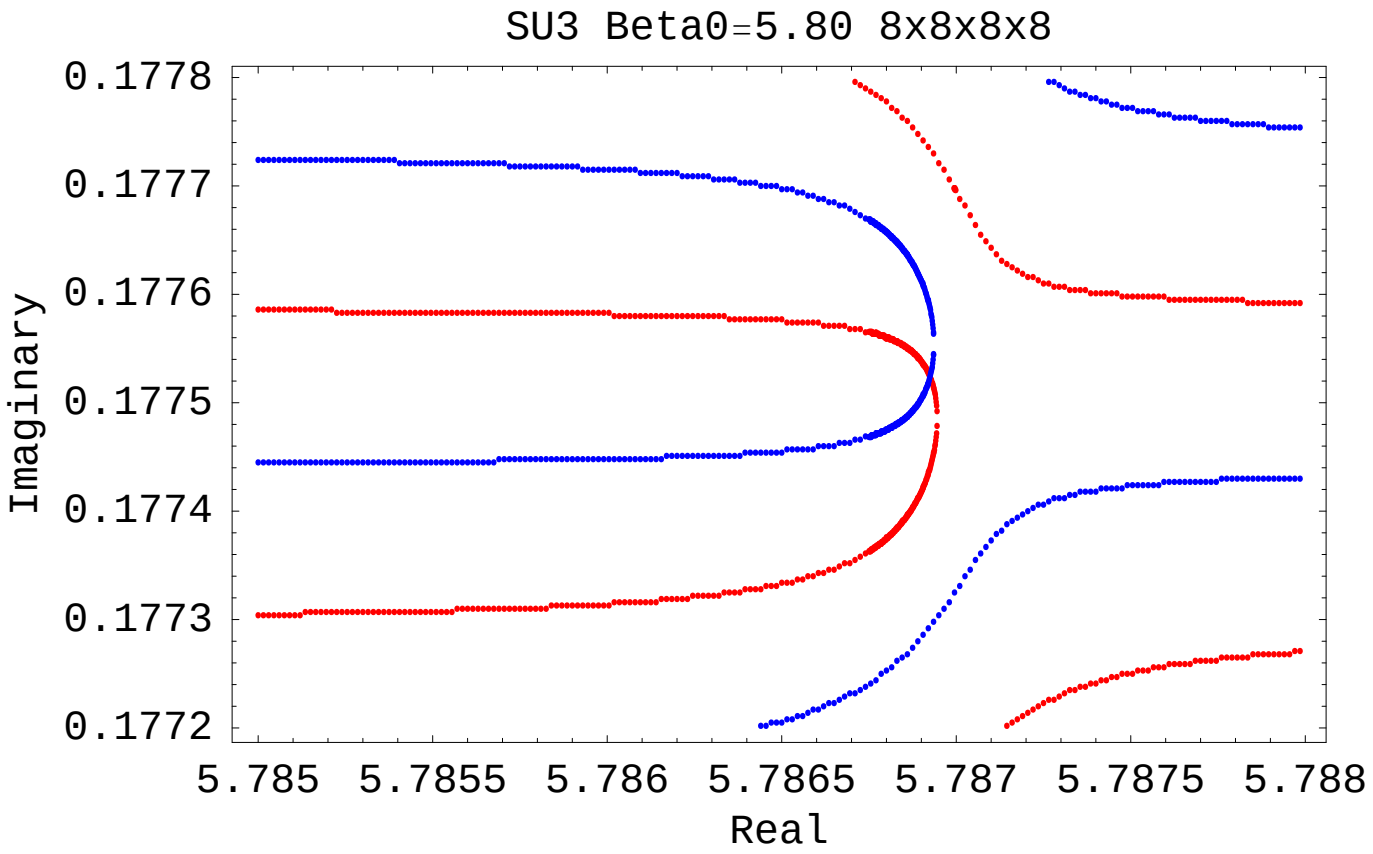

Figure 13: Zeroes of the real (blue) and imaginary (red) part of the partition function in the complex β plane (work done with Alan denBleyker).

The non-perturbative part of the plaquette

Objections: it depends on the order and the scheme

General statements:

Take a generic asymptotic series: $A \sim \sum_k a_k \lambda^k$

We assume that the error at order $k \ \simeq \lambda^{k+1} a_{k+1}$ (for λ small enough)

large order behavior: $|a_k| \sim C_1 C_2^k \Gamma(k + C_3)$

The error is minimized for $k^\star \simeq (\lambda C_2)^{-1} - C_3 - (1/2) + \mathcal{O}(1/k^\star)$

$Min_k \, |Error| \simeq \sqrt{2\pi} C_1 (\lambda C_2)^{1/2 - C_3} \mathrm{e}^{-\frac{1}{C_2 \lambda}}$ (order independent)

(Legendre transform in k; see Arnold Math. Meth. of Class. Mech. p. 63)

The anharmonic oscillator

$$H = p^2/2 + x^2/2 + \lambda x^4$$

$$E_0 \sim \sum_{k=0} a_k \lambda^k$$

$$a_k \sim (-1)^{k+1} \sqrt{6/\pi^3}\ 3^k\ \Gamma(k+1/2)$$ (Bender Wu 69)

$$Min_k\ |Error| \simeq (\sqrt{12}/\pi)\ \mathrm{e}^{-\frac{1}{3\lambda}}$$

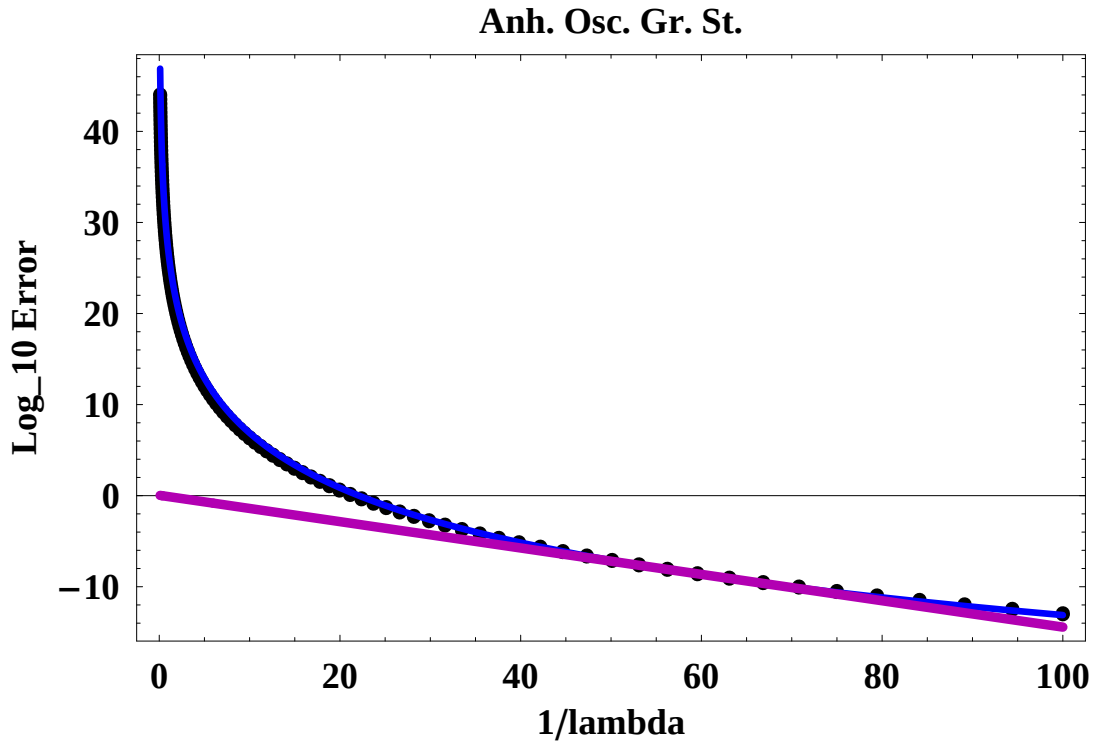

Figure 14: Difference between the perturbative series at order 19 and the numerical value of the ground state energy for the anaharmonic oscillator (in Log 10 scale). The blue line represents order 20. The purple line is the maximal accuracy estimated from the asymptotic behavior of the series.

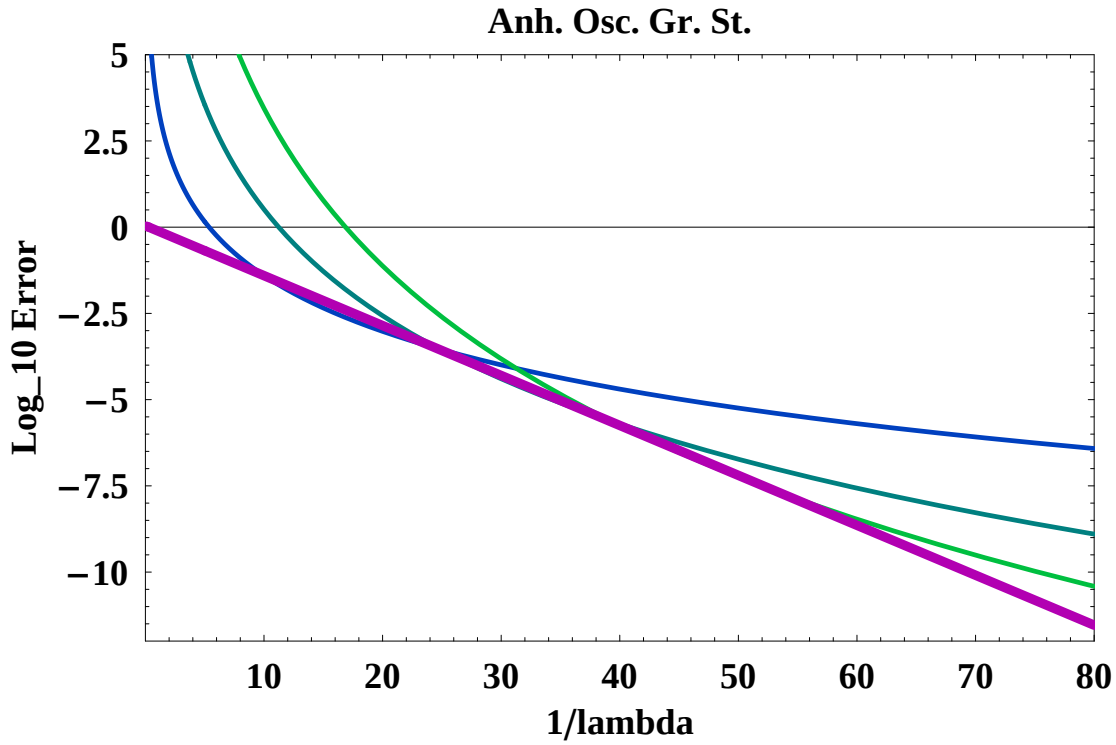

Figure 15: Difference between the perturbative series at order 5, 10 and 15 and the numerical value of the ground state energy for the anaharmonic oscillator (in a Log 10 scale). As the order increases, the curves get more green. The purple line is the maximal accuracy estimated from the asymptotic behavior of the series

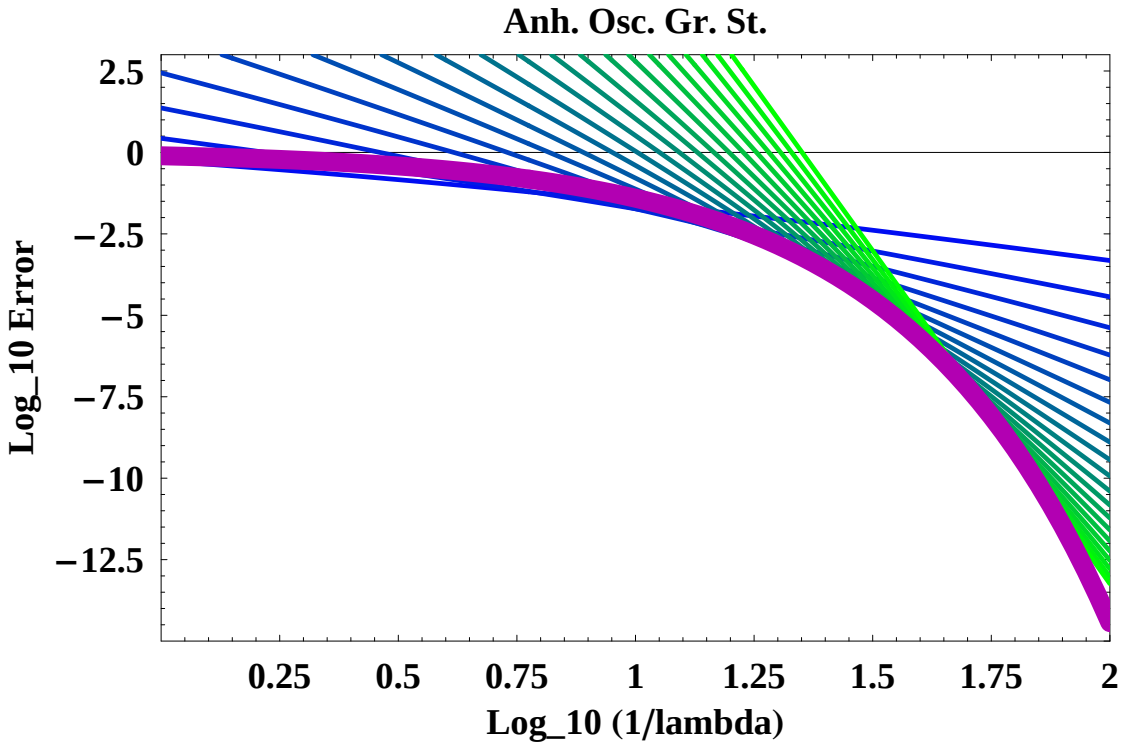

Figure 16: Difference between the perturbative series at order 1 to 20 and the numerical value of the ground state energy for the anaharmonic oscillator (in a Log 10 - Log 10 scale). As the order increases, the curves get more green. The purple line is the maximal accuracy estimated from the asymptotic behavior of the series

The double-well potential

In shifted coordinates, $V(y) = (1/2)y^2 - gy^3 + (g^2/2)y^4$.

$E_0 \sim \sum_{k=0} a_k \; g^{2k}$

$a_k \sim -(3/\pi) \; 3^k \; \Gamma(k+1)$ (Brezin, Parisi and ZJ, PRD 16 408 (1977))

$Min_k \; |Error| \simeq \sqrt{6/\pi} \; g^{-1} \; \mathrm{e}^{-\frac{1}{3g^2}}$

$\Delta E_0 = -(g\pi)^{-1/2} \; \mathrm{e}^{-\frac{1}{6g^2}}$ (1 instanton)

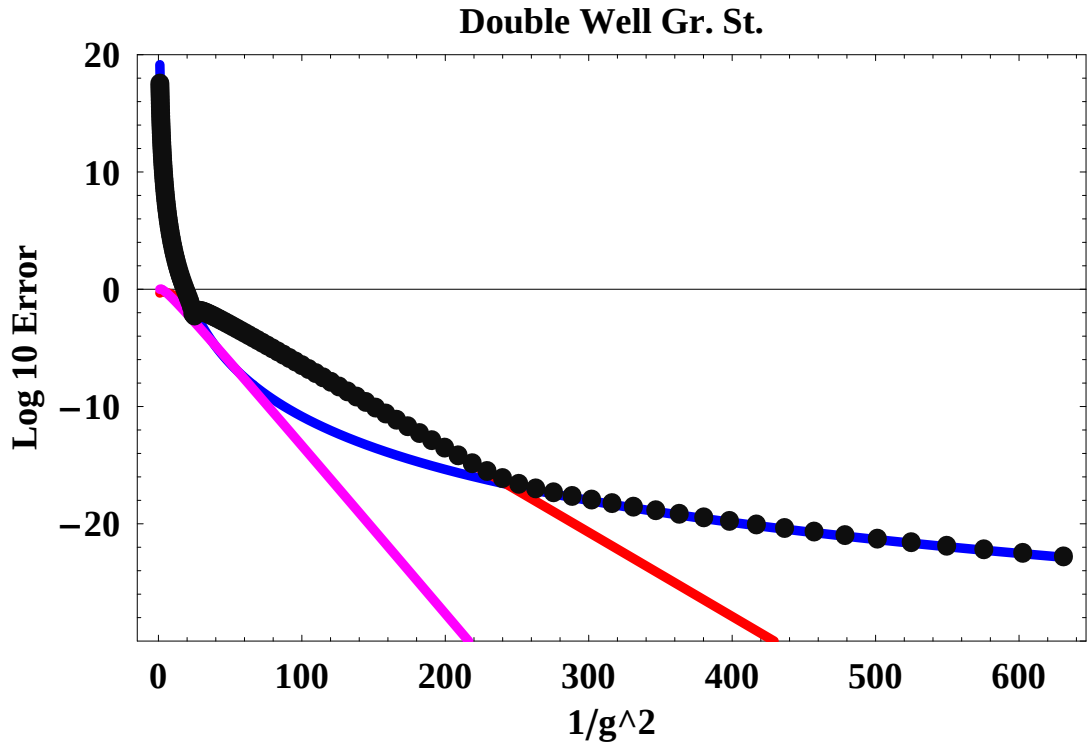

Figure 17: Difference between the perturbative series at order 28 and the numerical value of the ground state energy for the double-well (in Log 10 scale). The blue line represents order 30. The purple line is the maximal accuracy estimated from the asymptotic behavior of the series. The red line is the one instanton effect.

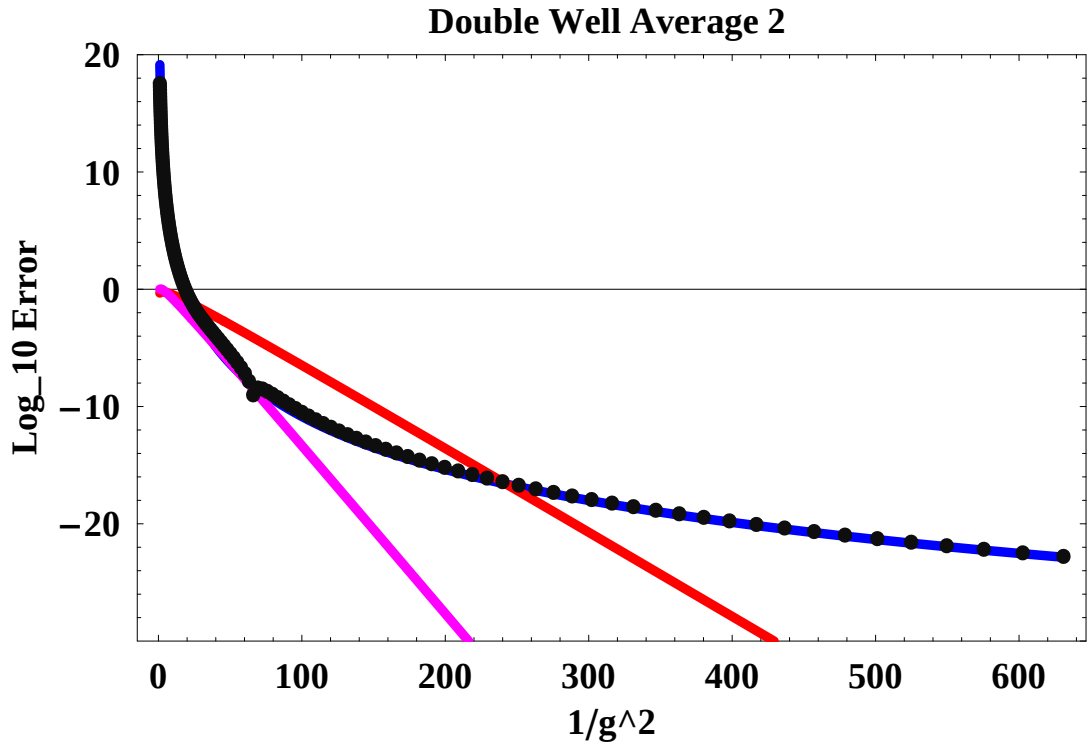

Figure 18: Difference between the perturbative series at order 28 and the average of the two lowest energy states for the double-well (in Log 10 scale). The blue line represents order 30. The purple line is the maximal accuracy estimated from the asymptotic behavior of the series. The red line is the one instanton effect

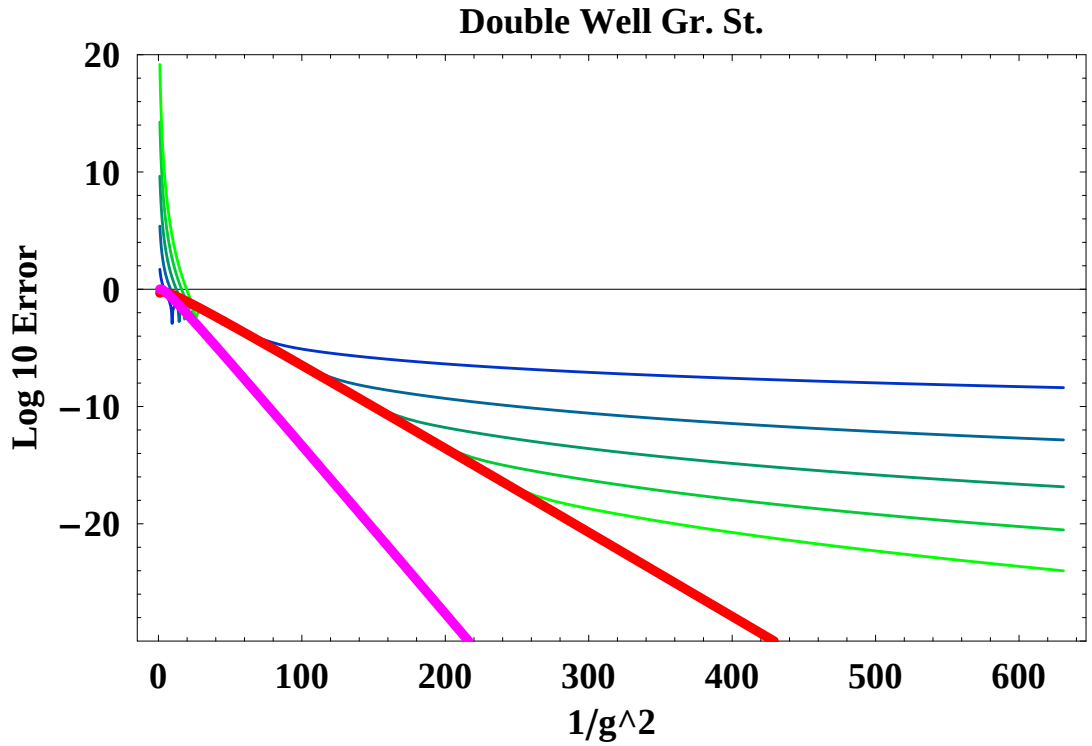

Figure 19: Difference between the perturbative series at order 6, 12, 18, 24 and 30 and the numerical value of the ground state energy for the double-well (in Log 10 scale). As the order increases, the curves get more green. The purple line is the maximal accuracy estimated from the asymptotic behavior of the series. The red line is the one instanton effect.

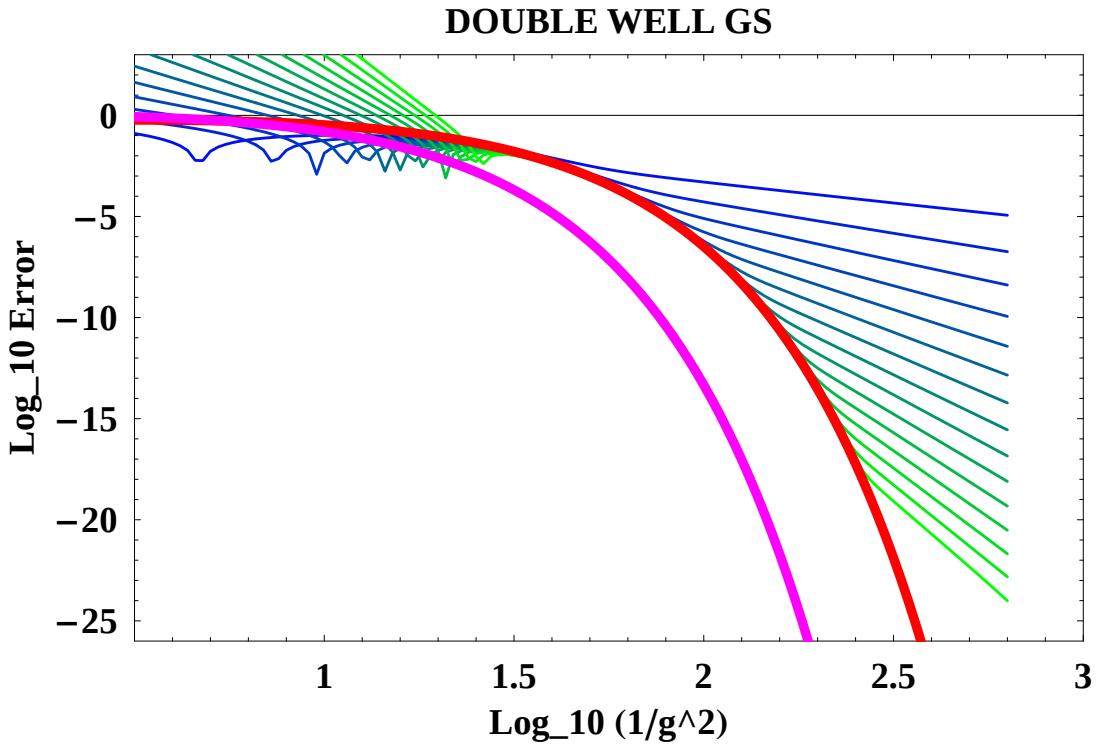

Figure 20: Difference between the perturbative series at order 2 to 30 and the numerical value of the ground state energy for the double-well (in a Log 10 - Log 10 scale). As the order increases, the curves get more green. The purple line is the maximal accuracy estimated from the asymptotic behavior of the series. The red line is the one instanton effect.

- We learned that there can be non-perturbative effects (here the one instanton effect), that cannot be guessed from the perturbative series.

- The error obtained from the perturbative series can rather be interpreted as an instanton-antiinstanton effect (see Brezin et al.)

- If we average over the two lowest eigenvalues, we cancel the one instanton effect and the error from the perturbative formula works.

a^4 versus a^2 controversy for $P_{NonPert.}$

$$P_{NonPert.} = (P - Series) \propto a^A \sim \left(\mathrm{e}^{-\frac{4\pi^2}{33}\beta} \right)^A ;$$

$A = 2$ (Burgio et al PLB 422) or 4 (Horsley et al Lattice 2001) ?

$A = 4$ corresponds to the perturbative envelope

$P_{NonPert.} \simeq 1.3 \times 10^{10} \ \ \mathrm{e}^{-\frac{16\pi^2}{33}\beta}$ (one-loop)

$P_{NonPert.} \simeq 1.6 \times 10^{8} \ (\frac{8\pi^2\beta}{33})^{\frac{204}{121}} \ \mathrm{e}^{-\frac{16\pi^2}{33}\beta}$ (two-loop)

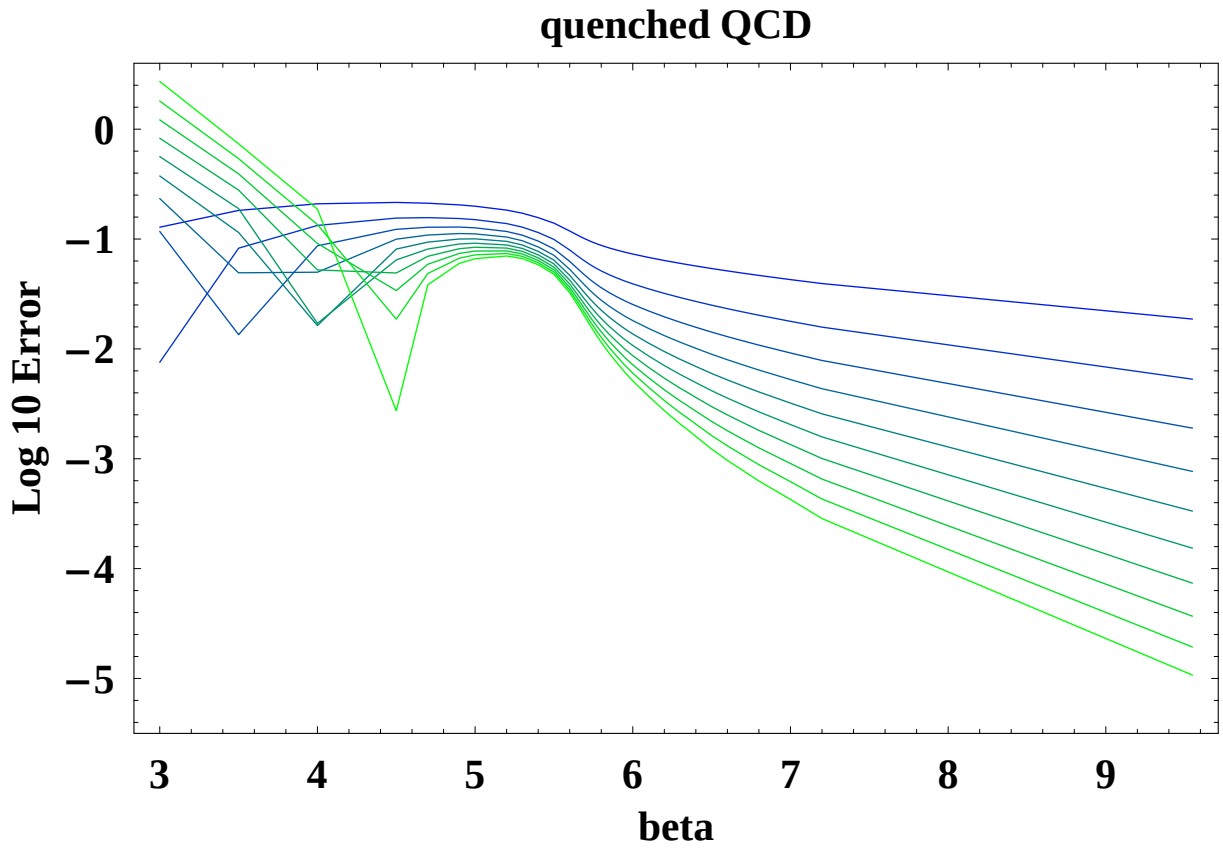

Figure 21: Difference between the perturbative series at order 1 to 10 and the numerical value of the plaquette (in Log 10 scale). As the order increases, the curves get more green.

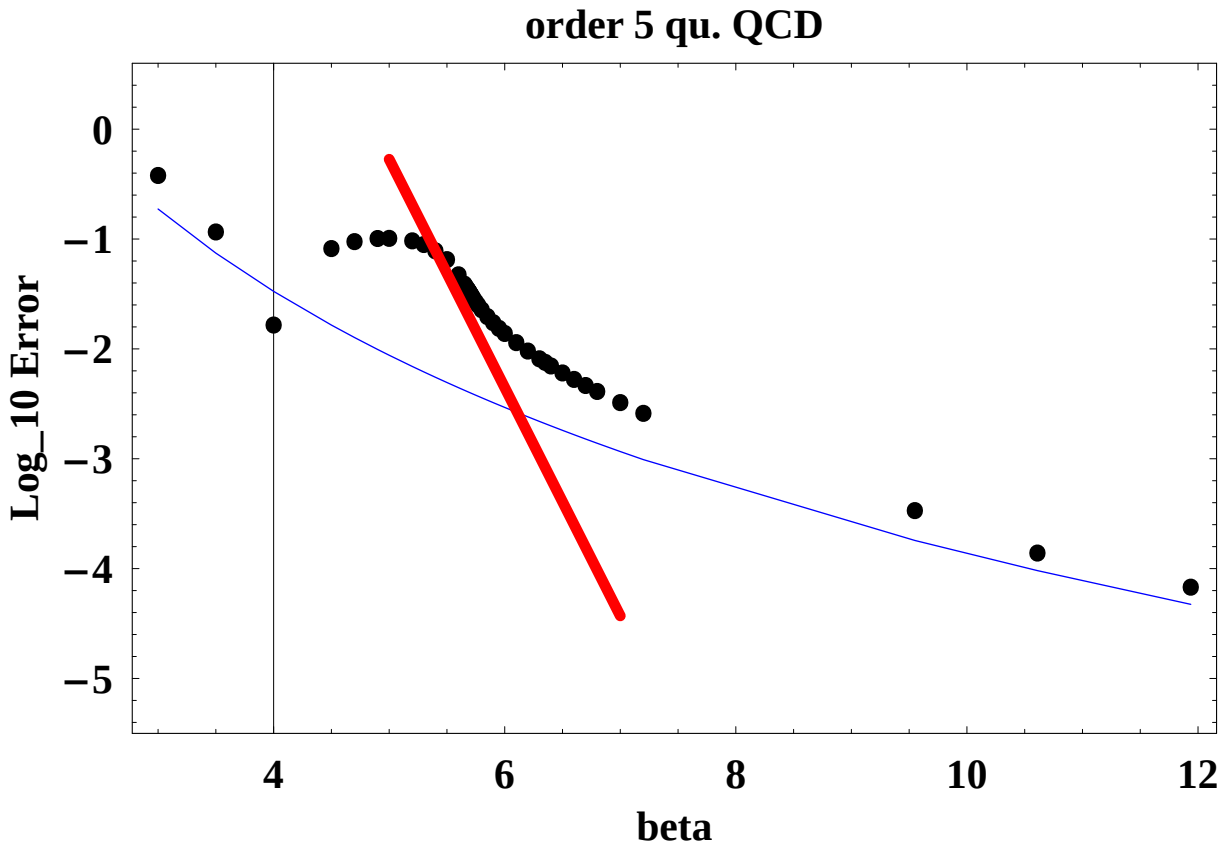

Figure 22: Difference between the perturbative series at order 5 and the numerical value of the plaquette (in Log 10 scale). The blue line is the order 6 contribution. The red line is $1.3 \times 10^{10} \times \mathrm{e}^{-\frac{16\pi^2}{33}\beta}$

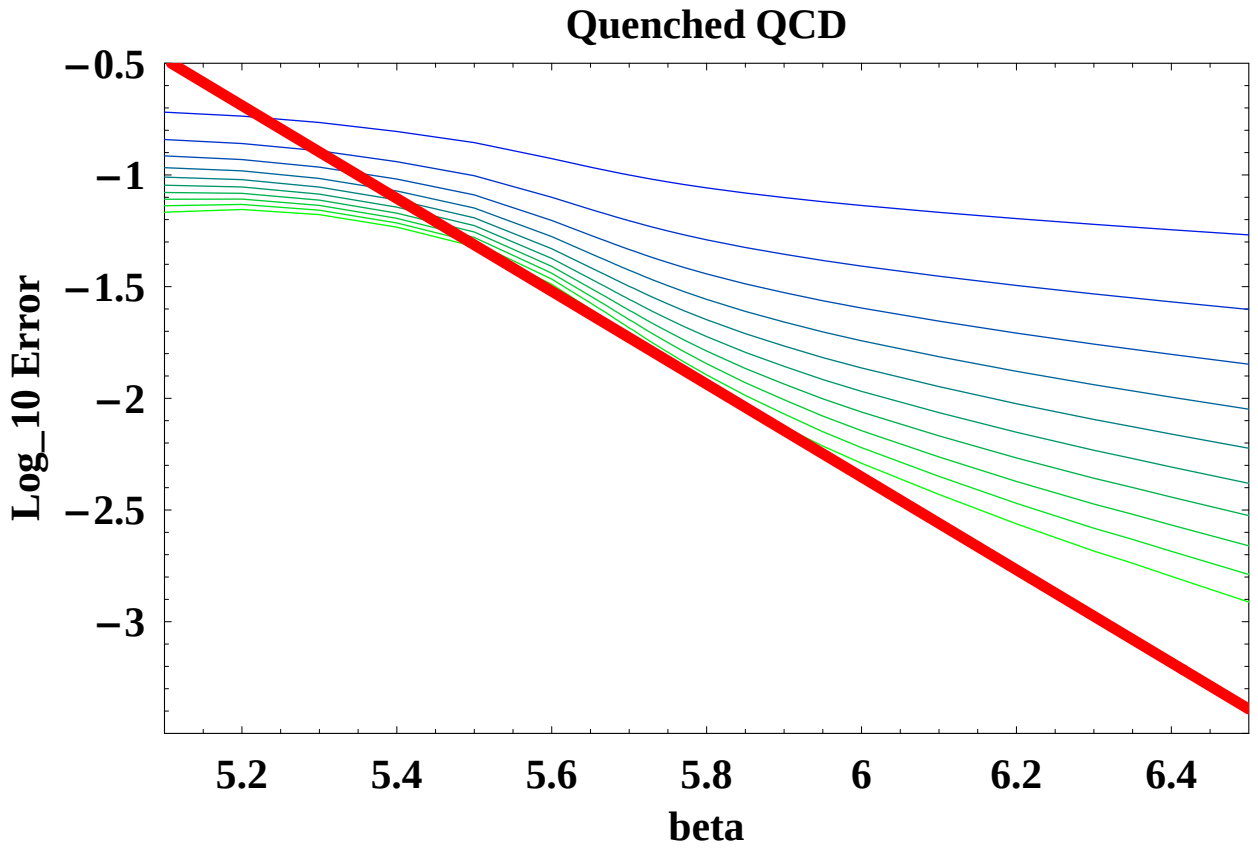

Figure 23: Difference between the perturbative series at order 10 and the numerical value of the plaquette (in Log 10 scale). The red line is $1.3 \times 10^{10} \times \mathrm{e}^{-\frac{16\pi^2}{33}\beta}$

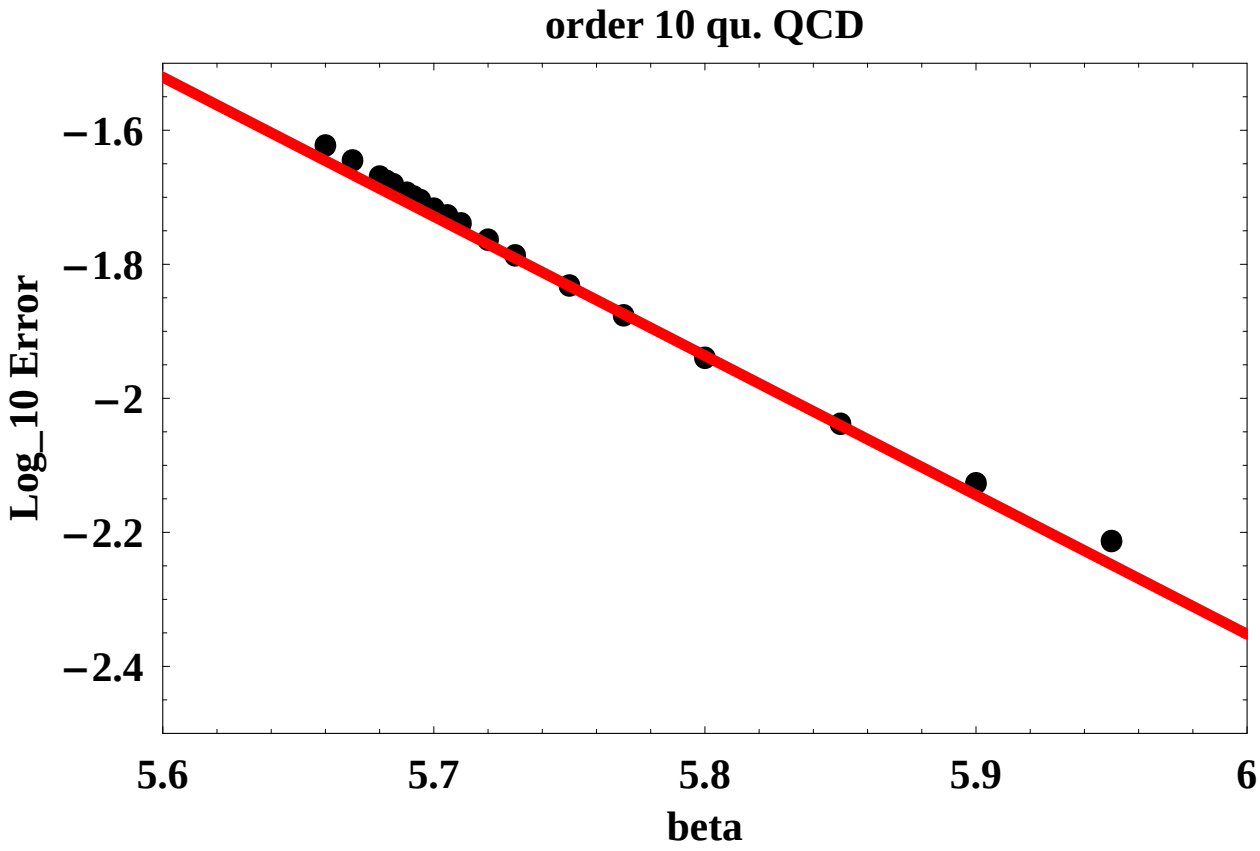

Figure 24: Difference between the perturbative series at order 10 and the numerical value of the plaquette (in Log 10 scale). As the order increases, the curves get more green.

Tadpole Improvement

$$P(1/\beta) \simeq \sum_{m=0}^{K} b_m \beta^{-m} = \sum_{m=0}^{K} e_m \beta_R^{-m} + O(\beta_R^{-K-1})$$

$$\beta_R^{-1} = \beta^{-1} \frac{1}{1 - \sum_{m=0} b_m \beta^{-m}}$$ (Lepage Mackenzie PRD 48)

Sommer's scale ($r_0 = 0.5$ fermi)

$$Ln(a/r_0) = -1.6805 - 1.7139(\beta - 6) + 0.8155(\beta - 6)^2 - 0.6667(\beta - 6)^3$$

(see also P. Rakow, Lattice 2005)

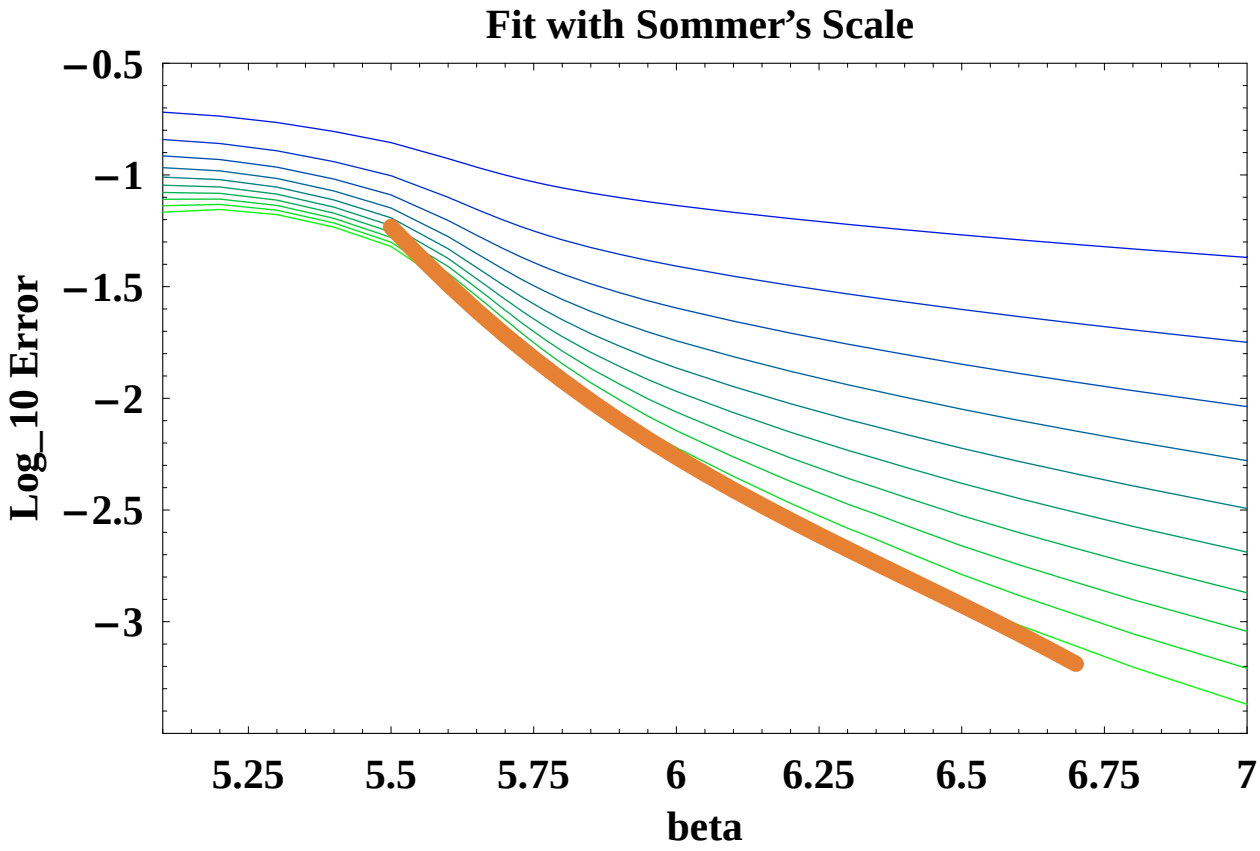

Figure 25: Difference between the perturbative series at order 1 to 10 and the numerical value of the plaquette (in Log 10 scale). As the order increases, the curves get more green. Fit with Sommer's scale (brown)

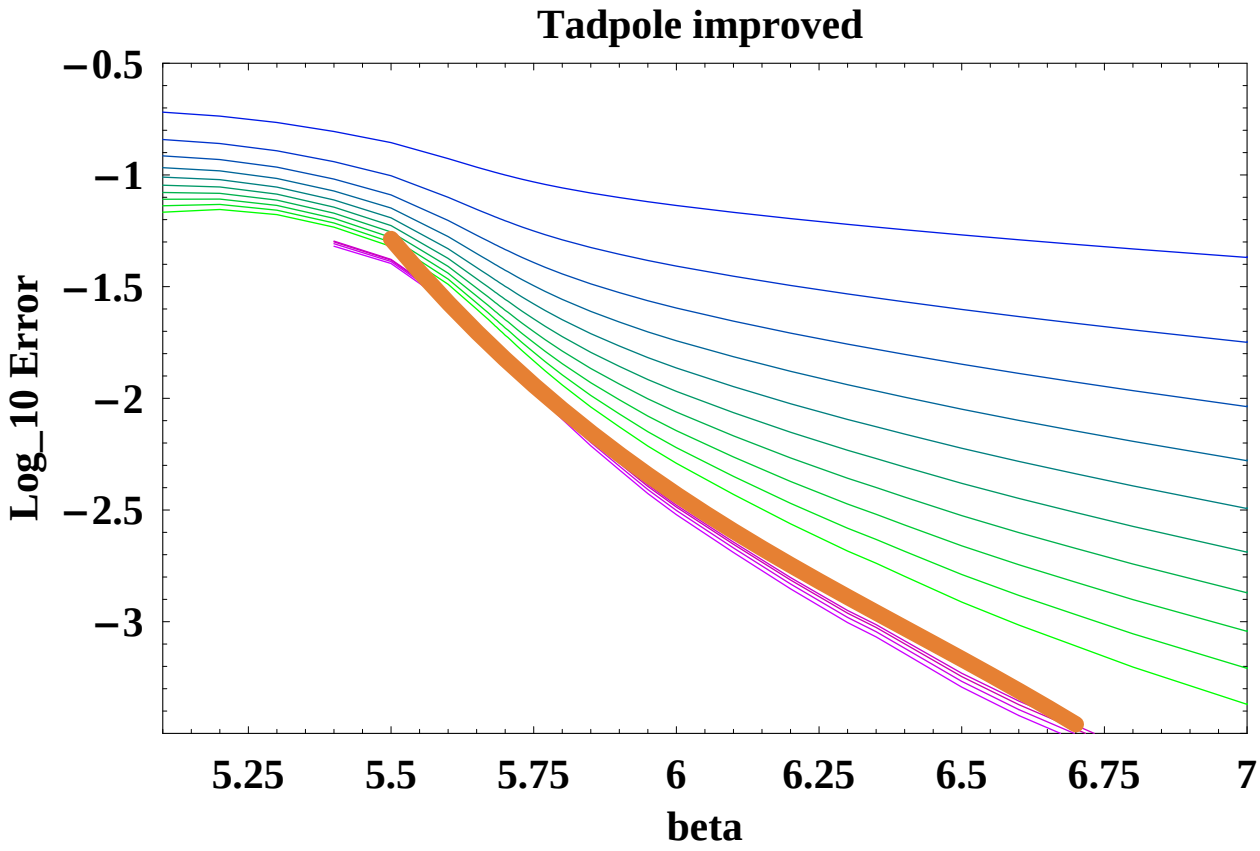

Figure 26: Difference between the perturbative series at order 1 to 10 and the numerical value of the plaquette (in Log 10 scale). As the order increases, the curves get more green. Tadpole imporved series at order 7 to 10 (purple) Fit with Sommer's scale (brown).

Work in progress

MC calculations of pert. coefficients

Stochastic quantization with a field cutoff

Dispersion relations

Semi-classical calculations of the non-perturbative amplitudes

Scaling variable calculation of the perturbative amplitude.

Conclusions

- A better control of perturbative series of the standard model is necessary
- A field cutoff drastically improve the asymptotic behavior of series
- The field cutoff can be chosen to minimize the discrepancy with the uncut theory (or by considerations regarding the validity of the effective theory, if applicable).
- There seems to be a connection between the crossover behavior of the perturbative coefficients and crossover behavior of RG flows.
- Analytic methods remain to be developed to estimate the various parameters determined empirically in lattice QCD